# Synchrotron x-ray diffraction studies of the structural properties of electrode materials in operating battery cells

T. R. Thurston[a] and N. M. Jisrawi[b]
*Department of Physics, Brookhaven National Laboratory, Upton, New York, 11973*

S. Mukerjee, X. Q. Yang, and J. McBreen
*Department of Applied Science, Brookhaven National Laboratory, Upton, New York, 11973*

M. L. Daroux and X. K. Xing
*Gould Electronics, Inc., Eastlake, Ohio 44095-4001*

(Received 14 March 1996; accepted for publication 26 April 1996)

Hard x rays from a synchrotron source were utilized in diffraction experiments which probed the bulk of electrode materials while they were operating *in situ* in battery cells. Two technologically relevant electrode materials were examined; an $AB_2$-type anode in a nickel–metal–hydride cell and a $LiMn_2O_4$ cathode in a Li-ion ''rocking chair'' cell. Structural features such as lattice expansions and contractions, phase transitions, and the formation of multiple phases were easily observed as either hydrogen or lithium was electrochemically intercalated in and out of the electrode materials. The relevance of this technique for future studies of battery electrode materials is discussed. © *1996 American Institute of Physics.* [S0003-6951(96)03127-0]

There is considerable technical interest in the behavior of electrode materials in operating battery cells. It is therefore surprising that most experimental data collected on battery cells to date is indirect, even though *in situ* x-ray diffraction experiments on the surfaces of electrodes inside operating cells were first done over 30 years ago.[1] Much of the difficulty in characterizing electrochemical systems *in situ* arises because most probes cannot penetrate the surrounding electrolyte and cell container materials efficiently. In battery systems where the bulk of the electrode incorporates hydrogen or lithium, however, an extra difficulty occurs because the probe must penetrate the entire electrode volume. This is because it is desirable to determine whether a phenomena arises from the passivation layer which accrues on the electrode surface or from the incorporation of the hydrogen or lithium into the bulk. One solution to this experimental problem is to use neutrons as a probe, since they are highly penetrating.[2] The main problem with this technique is that neutron beam access and fluxes are limited, so one cannot readily perform experiments under all the different conditions that can occur in an operating battery cell.

In this letter, we present the results of *in situ* x-ray diffraction experiments utilizing hard x rays from a synchrotron source. We demonstrate that this technique has great promise in battery research through experiments performed on two technologically relevant electrode materials; an $AB_2$ anode in a nickel–metal–hydride cell and a $LiMn_2O_4$ cathode in a Li-ion rocking chair cell. Structural features such as lattice expansions and contractions, phase transitions, and the formation of multiple phases were easily observed in operating electrochemical cells. Future structural studies should lead to insights on the origins of a variety of phenomena, such as the mechanisms of over-discharge/over-charge damage to an electrode, activation processes, and the effects of element substitution, for example.

The experiments were performed at a bending magnet port at the National Synchrotron Light Source, X27-A. The beam line was configured with no mirrors or other x-ray optical components upstream of the hutch, so the entire spectrum or x rays emitted from the synchrotron ring was available for experimental studies. The key aspect of the experimental apparatus is a monochromator utilizing a bent Si(111) crystal operating in a Laue (transmissions) geometry. This monochromator design is relatively new;[3] before these studies it had been used exclusively by the medical group at the National Synchrotron Light Source. The samples were mounted in a transmission geometry on a two circle goniometer, and a LiF (200) crystal was used as an analyzer. The x-ray energy was set at ~24.5 keV ($\lambda = 0.505$ Å), an energy where the x-ray penetration depth through nickel–metal–hydride alloys is typically $l \sim 50$ $\mu$m, and somewhat more for the Li-ion electrode materials. With samples that are $z = 0.5$ nm thick and $l = 50$ $\mu$m, the x-ray beam is attenuated by a factor of $e^{-z/l} \sim 10^{-5}$ in transmission through the sample, but we show below that with the high flux available at a synchrotron source, a reasonable counting rate is still obtainable. We emphasize that experiments performed in a transmission geometry probe the bulk of the electrode material. In contrast, the penetration depth into a nickel–metal–hydride alloy would typically be ~1 $\mu$m if a more conventional configuration (8 keV x rays scattering in a reflection geometry) were used. Thus, the passivation layer at the surface of the electrode will often dominate the signal in conventional synchrotron x-ray diffraction experiments.

The electrochemical cells used in this study were different for each electrode material studied. We briefly describe the nickel-hydride cell construction here; a more detailed description is given in Ref. 4. Sheets of nickel-metal-hydride anode and carbon cathode material were mounted on 5 cm×5 cm plates with a radiation grafted polyethylene/polyamide felt separator between them. Both electrodes were immersed in 6 molar KOH electrolyte solution contained by a Plexiglas casing sealed with o-rings. For the $LiMn_2O_4$ cathode study, a cell with approximate dimensions 2 cm × 3cm × 0.5 mm was manufactured by Gould electronics in a man-

[a]Electronic mail: tom@solids.phy.bnl.gov
[b]Permanent address: Dept. of Physics, Birzeit University, West Bank.

 0003-6951/96/69(2)/194/3/$10.00 © 1996 American Institute of Physics
Downloaded¬09¬Mar¬2011¬to¬129.10.187.55.¬Redistribution¬subject¬to¬AIP¬license¬or¬copyright;¬see¬http://apl.aip.org/about/rights_and_permissions

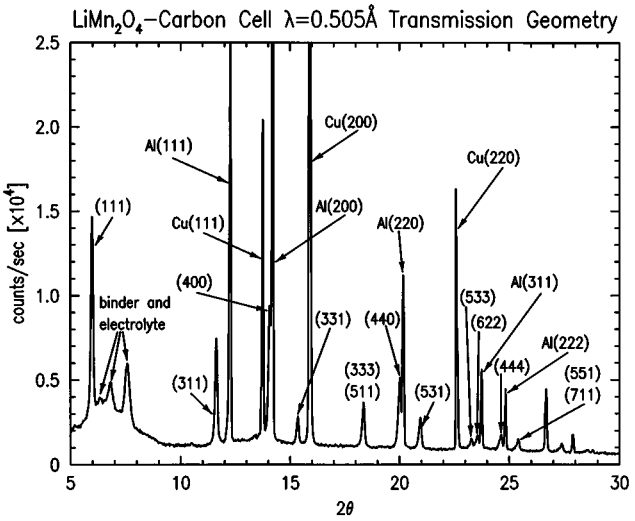


FIG. 1. $2\theta$ scan taken on a $LiMn_2O_4$-carbon cell when it was charged to 2.25 V. Peaks arising from aluminum, copper, binding materials, and the electrolyte are labeled. The rest of the indexed peaks are from the $LiMn_2O_4$ cathode material.

ner similar to commercial lithium-ion cells. A carbon anode and a proprietary nonaquaeous electrolye were utilized. The cell was sealed at the facory, and x-ray diffraction experiments were performed on it *with no modifications.*

In most secondary battery cells, a number of irreversible changes occur during the first few charging cycles. Examples of such phenomena include the formation of passivation layers on the electrode surfaces, and the fracture of grains within the electrodes. The process where a fresh cell is cycled until most irreversible changes stop occurring is called activation. In the present experiments, both cells were cycled/activated before x-ray diffraction studies were performed. The nickel–metal–hydride cell cycled ten times with a charging current of 4 mA and a discharging current of 3.5 mA. The cell was intentionally overcharged by ~20% during this procedure, and the potential ranged from ~0.7 V to ~1.4 V. The lithium-ion cell was cycled/activated between 2.6 and 4.3 V five times.

We first consider the $LiMn_2O_4$ cathode. This material is a promising candidate for use in the next generation of lithium ion rocking chair batteries since it is stable in air, easy to prepare, environmentally friendly, and considerably cheaper than the cathode materials currently in commercial use. There have been many structural studies[5] of $LiMn_2O_4$ but, to the best of our knowledge, only the measurements of Ohzuku, Kitagawa, and Hirai[5] were performed *in situ*, and these were done on a laboratory cell with a lithium–metal anode. In contrast, a rocking chair cell with a carbon anode comparable to commercial lithium-ion batteries was examined here. Figure 1 shows a $2\theta$ scan taken when the cell was charged to 2.25 V. We have indexed the $LiMn_2O_4$ peaks visible in Fig. 2 to a cubic cell (space group $Fd3m$); the other peaks labeled in Fig. 1 arise from copper, aluminum, binding materials, and the electrolyte. Scattering peaks from the carbon anode are *not* easily discernible in Fig. 1. For example, the (002) carbon peak should be at $2\theta \sim 8°$ at this x-ray energy. The electron density of carbon is too small and the anode material too disordered to allow this peak to be

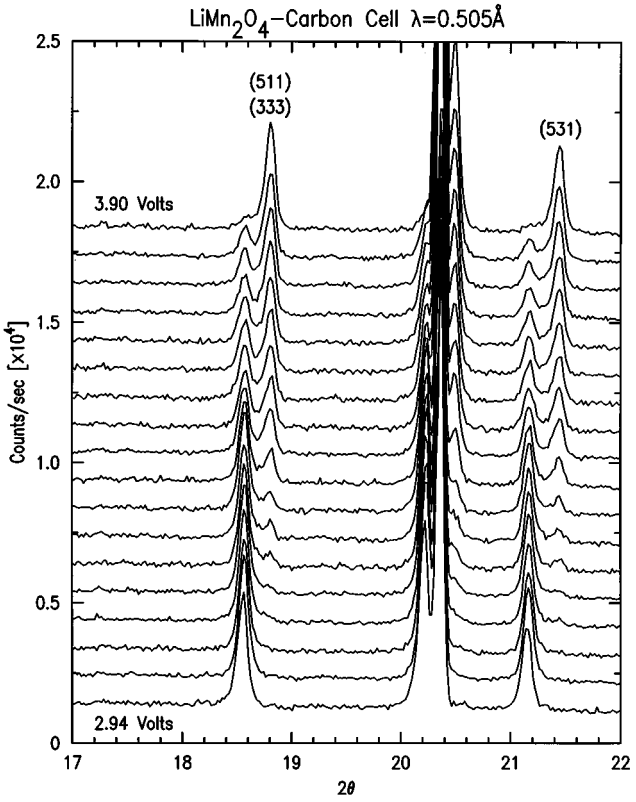


FIG. 2. Some $2\theta$ scans showing the evolution of the $LiMn_2O_4$ (511), (333), and (531) peaks as the cell is discharged from 3.90 to 2.94 V. The (440) peak at $\theta \sim 20.3°$ also evolves, but it is obscured by the aluminum (220) peak.

readily observable in this data set. We emphasize that the intensity of the largest $LiMn_2O_4$ peak, the (111) in Fig. 1, is ~12 000/s even though the cell was examined under *in situ* conditions. This counting rate is in fact comparable to those typically obtained in *ex situ* experiments on a conventional x-ray source. On the other hand, extraneous diffraction peaks and a diffuse background from the electrolyte and external cover of the cell can also be seen. The diffuse scattering is particularly large in the range of 5°–8°, but even at $2\theta$ angles greater than 20° the background intensity is ~500/s. Unfortunately, this background hinders detailed structural analysis somewhat, but it is unavoidable when performing *in situ* experiments.

An example of the structural information that can easily be obtained with this technique is illustrated in Fig. 2. Here $2\theta$ scans taken through the $LiMn_2O_4$ (511), (333), (440), and (531) peaks are presented [the (440) peak is partially obscured by an aluminum peak at 20.3°]. The data have been offset from each other for clarity, and they show the evolution of these peaks as the cell was discharged from 3.90 (top scan) to 2.94 V (bottom scan). During cell discharge, Li ions move out of the carbon anode and into the $LiMn_2O_4$ cathode. Although the small electron density of Li prevents one from directly observing Li intercalation peaks, the underlying $LiMn_2O_4$ lattice changes as Li is incorporated in the intercalation process. The data in Fig. 2 confirm this scenario, where analysis of the peak positions shows that the $LiMn_2O_4$ lattice constant expands from 8.03 to 8.18 Å as the cell is discharged, thus demonstrating that the Li intercala-


Downloaded¬09¬Mar¬2011¬to¬129.10.187.55.¬Redistribution¬subject¬to¬AIP¬license¬or¬copyright;¬see¬http://apl.aip.org/about/rights_and_permissions

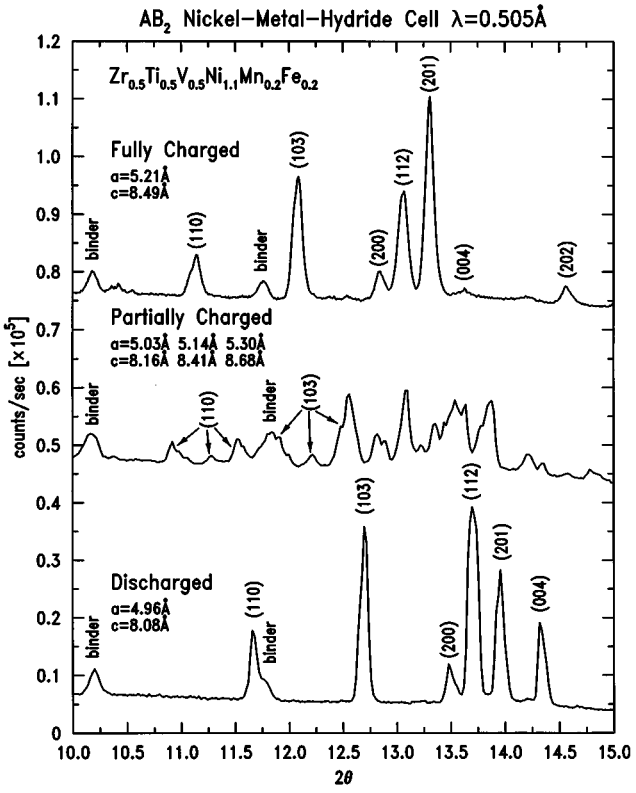


FIG. 3. Some $2\theta$ scans taken on an $AB_2$ nickel–metal–hydride cell at various charge states. Only one phase is present when the cell is fully charged or discharged, but in the partially charged state multiple phases with different hydrogen concentrations coexist.

tion process has been directly monitored. Our data also show that two cubic phases with different lattice constant values coexist in the transitional voltage range; we discuss this and other Li intercalation phenomena in $LiMn_2O_4$ electrodes in a subsequent publication.

We next consider the $AB_2$ nickel–metal–hydride material $Zr_{0.5}Ti_{0.5}V_{0.5}Ni_{1.1}Mn_{0.2}Fe_{0.2}$. This particular alloy composition was chosen for this demonstration experiment because it exhibits only one phase (hexagonal C14 Laves) in its unhydrided state.[6] The signal rate from more complicated multiphase nickel–metal–hydride materials will be comparable, however. Figure 3 shows $2\theta$ scans taken at various charge states of the cell. In the bottom scan the cell is discharged, in the second scan it is partially charged, and in the top scan it is fully charged. $AB_2$ peaks and peaks arising from the electrode binder material have been indexed in the scans. We emphasize that the intensities of the stronger $AB_2$ peaks in Fig. 3 are $\sim$30 000/s, so experiments on nickel–metal–hydride electrode materials can be routinely performed using this technique. As expected, the $AB_2$ unit cell volume expands dramatically ($\sim$16%) on hydrogen charging. Examination of the relative intensities of the (112), (201), and (004) peaks in the fully charged and discharged states also shows that the underlying metal lattice structure has been modified in accommodating the hydrogen.

In the scan taken on the partially charged state in Fig. 3, the structure is too disordered to index all of the peaks. Nonetheless, we tentatively identify six of the peaks with the (110) and (103) peaks of three hexagonal phases with different unit cell volumes. Interestingly, one of these coexisting phases has lattice constants larger than those of the phase present when the cell is fully charged. In experiments where hydrogen gas is charged into this material, the partially charged state typically exhibits two phase coexistence between high-hydrogen-density $\alpha'$ and low-hydrogen-density $\alpha$ structures. Our data on the partially charged state is similar to the gas phase data in some but not all respects. The differences in behavior have probably arisen either from macroscopic inhomogeneities in this particular electrode sample, or from the presence of a distribution of $AB_2$ grain sizes coupled with finite size effects.

The data presented above show that the bulk structural properties of electrode materials can be measured in operating electrochemical cells with hard x rays. We summarize here the advantages and disadvantages of the technique. The two major disadvantages are that the low electron density of hydrogen and lithium prevents one from monitoring the structural state of these key elements directly, and that the background signal from the electrolyte, binders, and other miscellaneous cell materials can be relatively large. The latter problem is unavoidable in any *in situ* scattering experiment on operating battery cells. The former problem can be circumvented if necessary by performing complementary neutron diffraction studies. On the other hand, there are unique advantages to using this technique. The experiments are easily performed, have a rapid data collection rate, and the design requirements for suitable electrochemical cells are relatively lax. Considering that there have been very few studies of the microscopic structural properties of operating electrodes to date, this technique should play a vital role in future battery research.

We wish to thank J. B. Hastings and D. P. Siddons of the NSLS beam line Research and Development group for making available generous amounts of beam time on X27A. This work was supported by the U.S. Department of Energy under Contract No. DE-AC02-76CH00016.

[1] G. W. D. Briggs, Electrochim. Acta **1**, 297 (1959); J. N. Andrews and A. R. Ubbelohde, Proc. Roy. So. London Ser. A **253**, 6 (1959); S. U. Falk, J. Electrochem. Soc. **107**, 661 (1960); G. W. D. Briggs and W. F. K. Wynne-Jones, Electrochim. Acta **7**, 241 (1962); A. J. Salkind and P. F. Bruins, J. Electrochem. Soc. **109**, 356 (1962); R. R. Chianelli, J. C. Scanlon, and B. M. L. Rao, J. Electrochem. Soc. **125**, 1563 (1978); M. Fleischmann and B. W. Mao, J. Electroanal. Chem. **229**, 125 (1987); M. G. Samant, M. F. Toney, G. L. Borges, L. Blum, and O. R. Melroy, Surf. Sci. **193**, L29 (1988); N. M. Jisrawi, H. Weismann, M. W. Ruckman, T. R. Thurston, G. Reisfeld, B. Ocko, and M. Strongin (unpublished).

[2] M. Latroche, A. Percheron-Guegan, Y. Chabre, C. Poinsignon, and J. Pannetier, J. Alloys Compd. **189**, 59 (1992).

[3] P. Suortti, W. Thomlinson, D. Chapman, N. Gmür, D. P. Siddons, and C. Schulze, Nucl. Instrum. Methods A **336**, 304 (1993). .

[4] S. Mukerjee, J. McBreen, J. J. Reilly, J. R. Johnson, G. Adzic, K. Petrov, M. P. S. Kumar, W. Zhang, and S. Srinivasan, J. Electrochem. Soc. **142**, 2278 (1995).

[5] M. H. Rossouw, A. de Kock, L. A. de Picciotto, M. M. Thackeray, W. I. F. David, and R. M. Ibberson, Mater. Res. Bull. **25**, 173 (1990); T. Ohsuku, M. Kitagawa, and T. Hirai, J. Electrochem. Soc. **137**, 769 (1990); M. M. Thackeray, A. de Kock, M. H. Rossouw, D. Liles, R. Bittihn, and D. Hoge, J. Electrochem. Soc. **139**, 363 (1992); J. M. Tarascon, W. R. McKinnon, F. Coowar, T. N. Bowmer, G. Amatucci, and D. Guyomard, J. Electrochem. Soc. **141**, 1421 (1994); A. Yamada, K. Miura, K. Hinokuma, and M. Tanaka, J. Electrochem. Soc. **142**, 2149 (1995); Y. Gao and J. R. Dahn, J. Electrochem. Soc. **143**, 100 (1996).

[6] J. Huot, E. Akiba, T. Ogura, and Y. Ishido, J. Alloys Compd. **218**, 101 (1995).


Downloaded¬09¬Mar¬2011¬to¬129.10.187.55.¬Redistribution¬subject¬to¬AIP¬license¬or¬copyright;¬see¬http://apl.aip.org/about/rights_and_permissions